

-*Supplementary information file-*

**Experimental and Theoretical Studies of Tetramethoxy-*p*-benzoquinone:
Infrared Spectra, Structural and Lithium Insertion Properties**

Gaëtan Bonnard,^a Anne-Lise Barrès,^b Yann Danten,^c Damian G. Allis,^d Olivier Mentré,^e Daniele Tomerini,^a Carlo Gatti,^f Ekaterina I. Izgorodina,^g Philippe Poizot^b and Christine Frayret^{a*}

^a LRCS-CNRS UMR 7314, Université de Picardie, 33, Rue Saint-Leu, 80039 Amiens, France

^b IMN-CNRS UMR 6502, Université de Nantes, 2, Rue de la Houssinière, 44322 Nantes, France

^c ISM-CNRS UMR 5255 , 351 Cours de la Libération, 33405 Talence, France

^d Department of Chemistry, Syracuse University, Syracuse, NY 13244, United States

^e UCCS, équipe de Chimie du Solide - CNRS UMR 8181, ENSC Lille-UST Lille, Cité Scientifique - Bât. C7 - BP 80108, 59655 Villeneuve d'Ascq cedex, France

^f CNR-ISTM, Istituto di Scienze e Tecnologie Molecolari, via Golgi 19, 20133, Milano, Italy

^g School of Chemistry, Monash University, Clayton, Victoria 3800, Australia

Contents

1. Computational details
2. Figures
3. Tables

1. Computational details

1.1 Bulk crystal modeling

In our simulations of TMQ and LiTMQ bulk crystals, we used three different DFT formalisms (*i.e.* the pseudopotential codes VASP¹ and CASTEP 6.01,² both based on a plane wave basis set and CRYSTAL09,^{3,4} a package that employs first principles DFT-LCAO). The search for the energetic minima of the two systems was carried out by varying atomic coordinates and lattice vectors simultaneously.

In the VASP calculations, we employed projector augmented-wave pseudopotentials (PAW)⁵ in which the semi-core states are treated as valence. An energy cut-off of 520 eV was applied. The Brillouin zone sampling was performed using the Monkhorst-Pack scheme⁶ with a k-points grid of 5x3x1. The structure was fully relaxed with the threshold of 10⁻⁵ eV for energy convergence and 10⁻³ eV/Å for residual forces. In order to take into account dispersion forces, we employed a semi-empirical method developed by Grimme⁷ that includes the long-range contributions via damped pairwise $f_{dmp}(R)C_6R^{-6}$ terms at a negligible cost compared to standard DFT calculations. Such corrections are introduced as:

$$E_{disp} = -s_6 \sum_{i=1}^{N-1} \sum_{j=i+1}^N \sum_g \frac{C_6^{ij}}{R_{ij,g}^6} f_{dmp}(R_{ij,g}) \quad (1)$$

where the energy is the summation over all atom pairs and g lattice vectors, N is the number of atoms, s_6 is a functional-dependent global scaling factor, C_6^{ij} is the dispersion coefficient of atom pair ij , and $R_{ij,g}$ is the inter-nuclear separation of the atom pair. The following damping function, f_{dmp} , is used in order to avoid near-singularities for small $R_{ij,g}$ values and double-counting effects of correlation at intermediate distances:

$$f_{dmp}(R_{ij,g}) = \frac{1}{1 + e^{-d(R_{ij,g}/R_r - 1)}} \quad (2)$$

where R_r is the sum of atomic vdW radii, R_{vdW} . This treatment (labeled PBE-D) has gained popularity, providing an improved description of molecular systems. However, Civalleri *et al.*^{8,9} demonstrated the need to adjust the parameterization (from PBE-D to PBE-D*) for the application of the method to crystalline solids. For PBE-D* parameterization,⁸ R_r is multiplied by 1.3 for H and by 1.05 for the other atoms. In previous works,¹⁰⁻¹² we observed a better

agreement between the optimized geometry using PBE-D* and experimental structures of lithiated organic crystals, although no complete transferability of the modified set was reached. In addition to the vdW radii modification, the s_6 value should also be adjusted in some cases.^{10, 12}

A hybrid HF-DFT method was also tested using the functional B3PW91¹³ provided by the CRYSTAL09^{3,4} package with the 6-31G(d,p) Gaussian-type basis set¹⁴⁻¹⁶ within the DFT-D2 treatment of Grimme. The Becke three-parameter hybrid functional (B3PW91) uses in the exchange part the mixture of the Fock (20%) and Becke (80%) exchange, whereas in the correlation part the Perdew-Wang (PWGGA) nonlocal correlation functional is employed^{17,18}. The SCF convergence threshold on the total energy was fixed at 10^{-12} Ha and the optimization convergence criterion on the RMS of the displacement at 10^{-3} eV/Å. Truncation criteria for bielectronic integrals (Coulomb and HF exchange series) were set to 10^{-7} , 10^{-7} , 10^{-7} , 10^{-7} , and 10^{-14} Hartree. 104101 total grid points were employed. A pruned (55,434) integration grid was used for the radial and angular distribution of grid points. Computations of harmonic normal modes and infrared intensity (IR) were conducted on the relaxed structure gained from the geometry optimization. Frequencies were determined by using weighted numerical evaluation of the Hessian matrix (the forces obtained were collected in a dynamical matrix where the eigenvalues give squared phonon frequencies and eigenvectors are equal to phonon modes).¹⁹ Infrared intensities were calculated by determining the Born effective charge tensor using a numerical evaluation of the well-localized Wannier functions of the unit cell.²⁰

A comparison between the Tkatchenko and Scheffler²¹ (TS) and Grimme methods was possible due to the implementation of the first method in the CASTEP 6.01² program. In the TS dispersion approach the C_6^{ij} coefficients and the vdW radii are not tabulated, but calculated values. The PBE exchange correlation functional was used in the calculation, and an energy cut-off of 700 eV was applied. The Brillouin zone sampling was performed using the Monkhorst-Pack scheme⁶ with a k-points grid of 6x3x2 (0.05 Å⁻¹ spacing in reciprocal space). The structure was fully relaxed with the threshold of 10^{-5} eV for energy convergence and 10^{-3} eV/Å for residual forces.

For the evaluation of the average potential value, a semi-empirical treatment of the dispersion was restricted to the lithiated or delithiated phases while bcc Li was treated with the PBE functional, as already mentioned in our previous works^{10,11}. Otherwise, as proven

from test calculations that we performed for the Li bcc metal in the PBE-D* treatment, geometry features are less close to the experimental one and the error generated in the estimation of the cohesive energy for this latter would affect the intercalation voltage estimation. Indeed, within the PBE-D* formalism, the relaxed a lattice parameter exhibits a discrepancy with respect to the experiment as large as - 6.7% (against - 2.05% for the PBE-D treatment).

1.2 Molecular/dimers modeling in gas phase

The optimized geometries issued from Gaussian-09 calculations²² for the isolated molecule and dimers of TMQ were obtained by using program option “tight” convergence criteria.

1.3 Madelung constants and lattice energies estimation

As in our previous work²³ only negative charges on oxygen atoms of the TMQ anion were included in the calculation of the Madelung constants for two structures of LiTMQ. The charges on oxygen atoms were augmented with fractional charges on the adjacent carbon atom(s). If the adjacent carbon atom belonged to the methyl group, the hydrogen charges were also added to those of the carbon atoms. For the second structure (less stable one) two out of six oxygen atoms on the anion turned out to have overall positive charge. These individual positive charges were then summed and equally shared with the rest of the oxygen atoms. As a result, only four oxygen atoms were included in the calculation of the Madelung constant for the less stable LiTMQ structure.

The Madelung constants of individual cation/anion in the unit cell was calculated using the following expression:

$$M_{ion} = N_{ion}^{salt} \frac{\sum_{i=1}^{N_{tot}} M_{ion}^i}{N_{tot}} \quad (3)$$

where ion is either cation or anion

N_{ion}^{salt} is stoicheometric coefficient of the cation/anion in the salt

N_{tot} is the total number of positively/negativel y charged atoms on the cation/anion

M_{ion}^i is individual Madelung constants of either positively charged atoms on the cation or negatively charged atoms on the anion

The normalised Madelung constant of the salt was calculated simply as:

$$M_{salt} = \frac{1}{2 \cdot Q_{tot}^2} (M_{cation} + M_{anion}) \quad (4)$$

where $\frac{1}{Q_{tot}^2}$ is the normalization factor converting fractional overall charge on ions to unity charge
 Q_{tot} is the total charge on each ion

The normalization in equation (4) was performed to allow for direct comparison with Madelung constants of inorganic salts reported in the literature.

The electrostatic lattice (E_{Lat}) energies were calculated as previously reported²³ using the unnormalized Madelung constant of the salt (i.e. excluding the $\frac{1}{Q_{tot}^2}$ -factor in equation (4) in E_{Lat}). The normalization was excluded from the calculation of the lattice energy to account for fractional (*i.e.* $< |1|$) charges on both cation and anion.

1.3 π electron delocalization indices : HOMA and FLU

Cyclic compounds with alternating single and double bounds tend to present intermediate bond lengths between those compounds with isolated single and/or double bonds. This property is a cooperative effect of both the σ and π orbitals. The harmonic oscillator model of aromacity (HOMA model) is a quantitative descriptor of this effect (geometric criterion) that allows a quantitative measure of the aromaticity of organic compounds. HOMA is defined as a normalized sum of squared deviations of the individual experimental (or calculated) bond lengths and an optimal bond length, which corresponds to full π -electron delocalization.

$$HOMA = 1 - \frac{1}{N} \sum_{i=1}^N \alpha_i (R_{opt} - R_i)^2 \quad (5)$$

where N is the number of bonds taken into the summation; α is a normalization constant (for CC bonds $\alpha = 257.78$; for CO bonds $\alpha = 157.38$) fixed to give HOMA = 0 for a model

nonaromatic system (*e.g.* the Kekulé structure of benzene)²⁴ and HOMA = 1 for the system with all bonds equal to the optimal value R_{opt} (*e.g.* a full aromatic system - for CC bonds R_{opt} is equal to 1.388 Å; for CO bonds R_{opt} is equal to 1.265 Å); R_i stands for a running bond length.

The analysis of the delocalization in the ring through HOMA has been complemented with the calculation of the fluctuation index of aromaticity (FLU),^{25,26} which measures the amount of electron sharing between contiguous atoms. Its expression is correlated to the two-center delocalization indices (DIs), $\delta(A,B)$, defined by Bader and co-workers^{27,28} that were calculated from the double integration of the exchange-correlation density over the atomic basins. The term $\delta(A,B)$ represents the extent of the correlative interaction between electrons into different regions quantitatively independent of the nature of the interaction.²⁹ The aromaticity fluctuation index (FLU) is thus defined as the deviation from the delocalization of electronic charge $\delta(A,B)$ over a bond in a ring composed of N atoms according to:

$$FLU = \frac{1}{N} \sum_{A,B}^{\text{bonds}} \left[\frac{\max(V(A),V(B))}{\min(V(A),V(B))} \left(\frac{\delta(A,B) - \delta_{\text{ref}}(A,B)}{\delta_{\text{ref}}(A,B)} \right) \right]^2 \quad (6)$$

where $V(A)$ is defined as the valence of an atom in AIM theory terms, the sum of the delocalization indexes of the atom A over all the other atoms and $\delta_{\text{ref}}(A,B)$ is a standardized value of delocalization for an aromatic bond. Value $\delta_{\text{ref}}(A,B)$ can be obtained as the delocalization in a C-C bond at the desired SCF level of theory. In this work it is taken as 1.389.

2. Figures

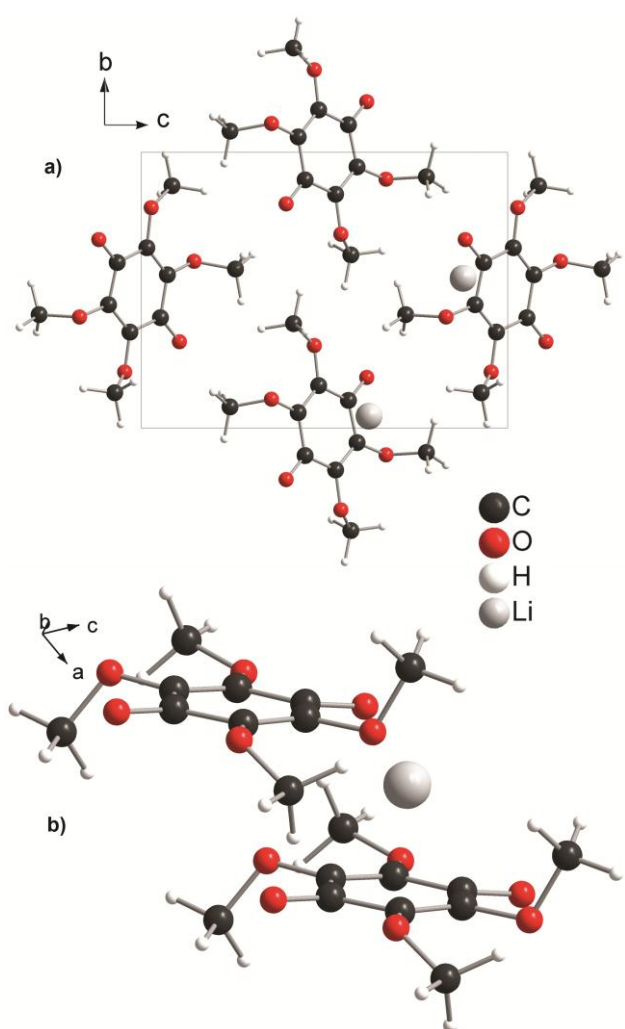


Fig. S1 Crystal structure of the most unstable relaxed model for the LiTMQ compound. a) View along the *a*-axis ; b) View showing the positioning of lithium in between the two molecules.

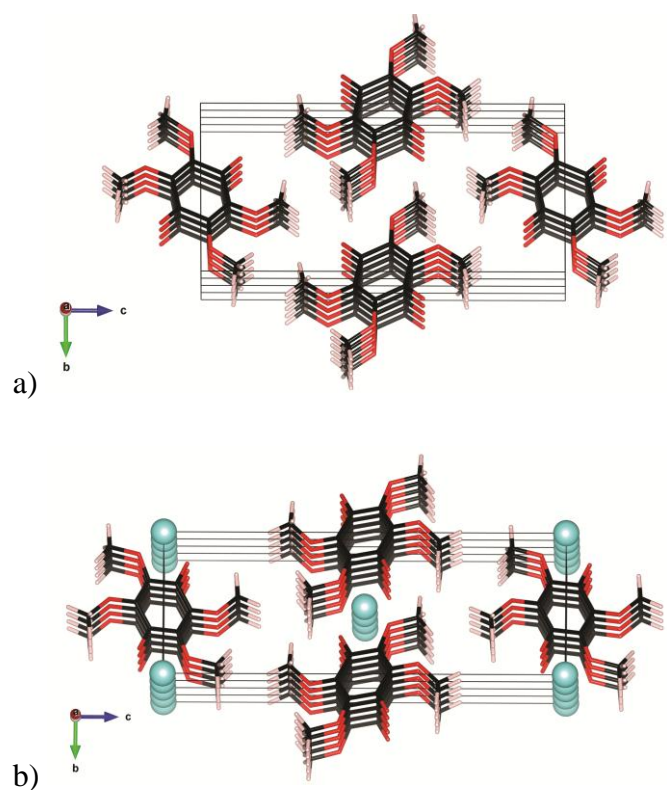


Fig. S2 : Crystal packing viewed down the *a*-axis for a) TMQ and b) most stable relaxed form of LiTMQ.

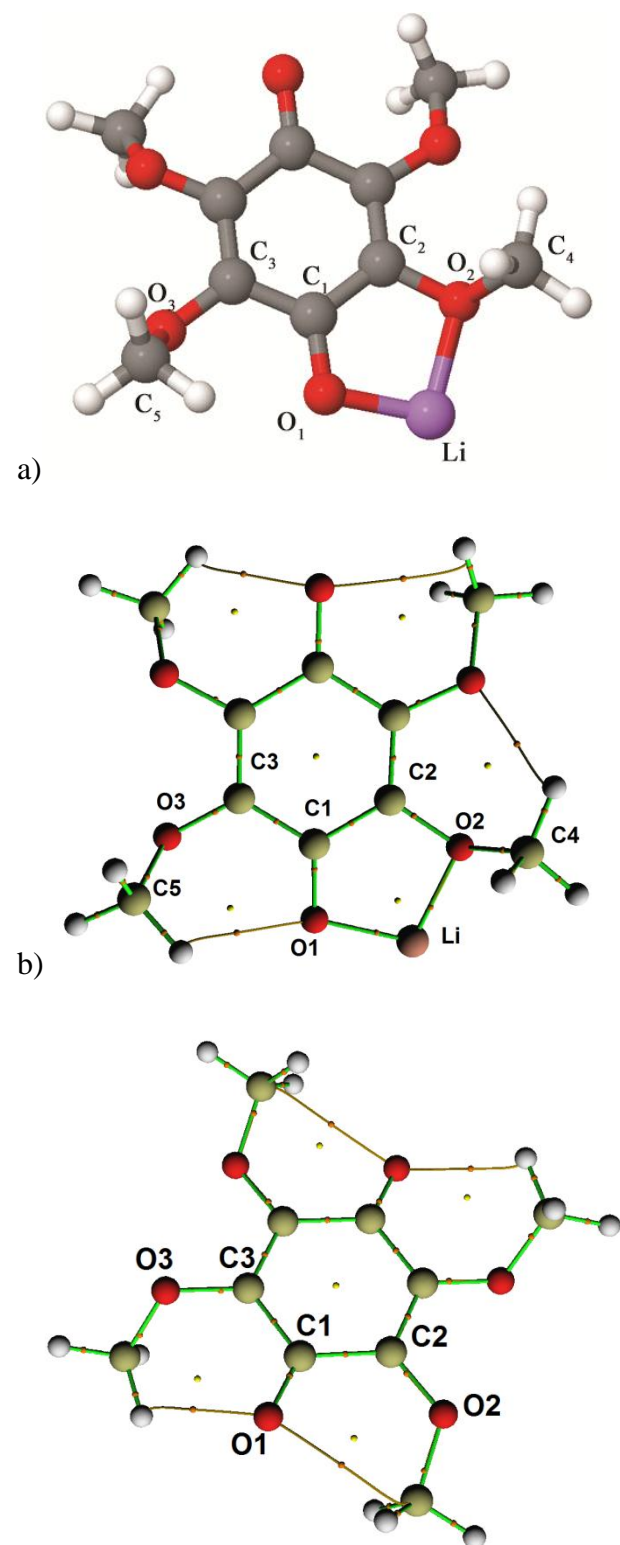


Fig. S3 a) Bond labelling in the Li^+ , TMQ^- complex (slight differentiation of bond lengths are not reported for the sake of simplicity and to facilitate data comparison between various systems); b) Bond critical points (small red spheres), ring critical points (small yellow sphere), bond paths (pink lines) in TMQ (above)/ Li^+ , TMQ^- (below) systems.

3. Tables

		<i>a</i> (Å)	<i>b</i> (Å)	<i>c</i> (Å)	β (°)	<i>V</i> (Å ³)	<i>d</i> (Å)
RT	Exp	4.0075(2)	7.7425(4)	16.7724(6)	94.112(3)	519.08(4)	3.46
	rev-PBE	4.9780	7.7020	17.9380	97.49	681.79	4.28
		+24.20%	-0.52%	+6.95%	+3.59%	+31.34%	+23.70%
	PBE	4.4245	7.6337	17.3042	96.43	580.78	3.87
		+10.41%	-1.41%	+3.17%	+2.46%	+11.89%	+11.85%
	LDA	3.6246	7.5408	16.0604	92.15	438.66	3.15
		-9.55%	-2.61%	-4.25%	-2.08%	-15.49%	-8.96%
	PBE-D	3.7251	7.7374	16.3865	93.02	471.64	3.22
		-7.05%	-0.07%	-2.30%	-1.16%	-9.14%	-6.94%
	PBE-D*	3.8956	7.6848	16.6729	93.45	498.23	3.36
		-2.79%	-0.75%	-0.59%	-0.71%	-4.02%	-2.89%
100 K	corr-PBE-D*_0.52 6-31G**	3.9330	7.6279	16.7561	93.99	501.47	3.36
		-1.87%	-1.34%	-0.04%	-0.13%	-3.39%	-2.89%
	PBE+TS	3.9137	7.7076	16.8607	94.68	506.90	3.41
		-2.36%	-0.46%	+0.53%	+0.60%	-2.35%	-1.51%
	PBEsol	4.0288	7.6070	16.7900	94.82	512.74	3.55
	corr-B3PW-D*_0.52 6-31G**	4.0167	7.6457	16.7967	96.23	512.79	3.48
		+0.22%	-1.24%	+0.15%	+2.50%	-1.21%	+0.44%
	corr-PBE-D*_0.52	4.0049	7.6938	16.8326	94.04	517.38	3.49
		-0.06%	-0.63%	+0.36%	-0.08%	-0.33%	+0.86%
	Exp	3.9137	7.7232	16.6264	93.41	501.66	3.33
	corr-PBE-D*_0.70	3.9150	7.6919	16.7042	93.57	502.05	3.36
		+0.03%	-0.41%	+0.47%	+0.17%	+0.08%	+0.85%

Table S1: Optimized lattice parameters, *a*, *b*, *c*, and β monoclinic angle, unit cell volume, *V*, and inter-plane distance, *d*, for TMQ at RT and 100 K by using various methods of calculations. Discrepancies with the experiment are indicated in bold.

EXP	Theoretical calculation		
	RT	from VASP corr-PBE-D*_0.52 (Å)	from CRYSTAL09 corr-B3PW91-D*_0.52 (Å)
<i>d(C-C)</i>			
<i>d(C₁-C₂)</i>	1.501	1.512	1.509
<i>d(C₂-C₃)</i>	1.343	1.370	1.362
<i>d(C₃-C₁)</i>	1.471	1.467	1.468
<i><d(C-C)></i>	1.438	1.450	1.446
<i>d(C-O)</i>			
<i>d(C₄-O₂)</i>	1.443	1.452	1.439
<i>d(C₅-O₃)</i>	1.427	1.450	1.436
<i>d(C₁-O₁)</i>	1.213	1.240	1.227
<i>d(C₂-O₂)</i>	1.339	1.334	1.324
<i>d(C₃-O₃)</i>	1.370	1.372	1.362
<i><d(C-O)></i>	1.358	1.370	1.358
<i>RMSD (C-C , C-O)</i>		0.017	0.011
<i>d(C-H)</i>			
<i>d(C4-H_{4a})</i>	0.960	1.094	1.088
<i>d(C4-H_{4b})</i>	0.961	1.096	1.090
<i>d(C4-H_{4c})</i>	0.960	1.094	1.089
<i>d(C5-H_{5a})</i>	0.960	1.096	1.090
<i>d(C5-H_{5b})</i>	0.959	1.099	1.093
<i>d(C5-H_{5c})</i>	0.960	1.098	1.093
<i><d(C-H)></i>	0.960	1.096	1.091
<i>d(C^{methyl}...H)</i>			
<i>d(O1...H5a)</i>	2.576	2.397	2.390
<i>d(O1...H4a)</i>	2.583	2.394	2.411
<i>d(O1...H5b)</i>	2.846	2.829	2.669
<i>d(O2...H4a)</i>	2.719	2.553	2.429
<i>d(O3...H5b)</i>	2.664	2.549	2.506
<i><d(C^{methyl}...H)></i>	2.678	2.544	2.481

Table S2 : Theoretically and experimentally determined intramolecular bond distances for the TMQ crystal at the corr-PBE-D*_0.52 and corr-B3PW91-D*_0.52/6-31G(d,p) levels of theory.

Coordinates	calc. values (Å)
C=O	1.218
C=C	1.355
C-C	1.476
C-O _(CH₃)	1.346
C $\ddot{\text{O}}$ O _(CH₃)	1.333
-O-C _(CH₃)	1.426
$\ddot{\text{O}}$ O-C _(CH₃)	1.429
O=C-C-	120.6
C-C-O _(CH₃)	118.7
C-C $\ddot{\text{O}}$ O _(CH₃)	118.9
O=C-C $\ddot{\text{O}}$	120.3
C-O-C _(CH₃)	117.5
C $\ddot{\text{O}}$ O-C _(CH₃)	122.1

Table S3: Optimized geometrical parameters (bond length and bond angles) of isolated TMQ in gas phase calculated at the B3PW91/6-311+G(2d,p) level.

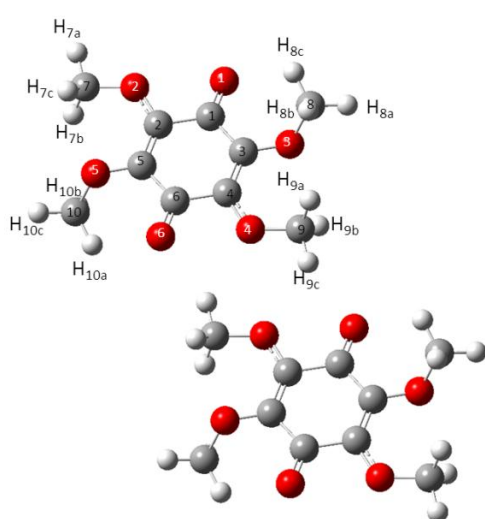
a)

	EXP	B3PW91/6-311+G(2d,p)	
	RT	Dimer 1	Dimer 2
<i>d(C-C) bonds</i> (Å)			
<i>d</i> (C ₁ -C ₂)	1.501	1.507	1.507
<i>d</i> (C ₁ -C ₃)	1.471	1.472	1.473
<i>d</i> (C ₂ =C ₅)	1.343	1.354	1.354
<i>d</i> (C ₃ =C ₄)	1.343	1.356	1.355
<i>d</i> (C ₄ -C ₆)	1.501	1.505	1.502
<i>d</i> (C ₆ -C ₅)	1.471	1.472	1.473
<i>d(C-O) bonds</i> (Å)			
<i>d</i> (C ₁ =O ₁)	1.213	1.214	1.213
<i>d</i> (C ₂ -O ₂)	1.339	1.325	1.326
<i>d</i> (C ₃ -O ₃)	1.370	1.356	1.355
<i>d</i> (C ₄ -O ₄)	1.339	1.324	1.326
<i>d</i> (C ₅ -O ₅)	1.370	1.358	1.359
<i>d</i> (C ₆ =O ₆)	1.213	1.216	1.216
<i>d</i> (C ₇ -O ₂)	1.443	1.423	1.423
<i>d</i> (C ₈ -O ₃)	1.427	1.426	1.431
<i>d</i> (C ₉ -O ₄)	1.370	1.359	1.427
<i>d</i> (C ₁₀ -O ₅)	1.370	1.359	1.426
<i>d(C-H) bonds</i> (Å)			
<i>d</i> (C ₇ -H _{7a})	0.960	1.089	1.089
<i>d</i> (C ₇ -H _{7b})	0.961	1.092	1.092
<i>d</i> (C ₇ -H _{7c})	0.960	1.089	1.089
<i>d</i> (C ₈ -H _{8a})	0.960	1.089	1.089
<i>d</i> (C ₈ -H _{8b})	0.959	1.096	1.094
<i>d</i> (C ₈ -H _{8c})	0.960	1.090	1.090
<i>d</i> (C ₉ -H _{9a})	0.960	1.088	1.089
<i>d</i> (C ₉ -H _{9b})	0.959	1.092	1.090
<i>d</i> (C ₉ -H _{9c})	0.960	1.089	1.089
<i>d</i> (C ₁₀ -H _{10a})	0.960	1.089	1.089
<i>d</i> (C ₁₀ -H _{10b})	0.961	1.096	1.096
<i>d</i> (C ₁₀ -H _{10c})	0.960	1.090	1.090
<i>Inter. distances</i> (Å)			
<i>R</i> _{cm1-cm2}		8.8 (8.72)	6.0 (4.01)
<i>Δxij</i>		8.5 (8.42)	4.6 (1.87)
<i>Δyij</i>		2.1 (2.19)	0.9 (0.68)

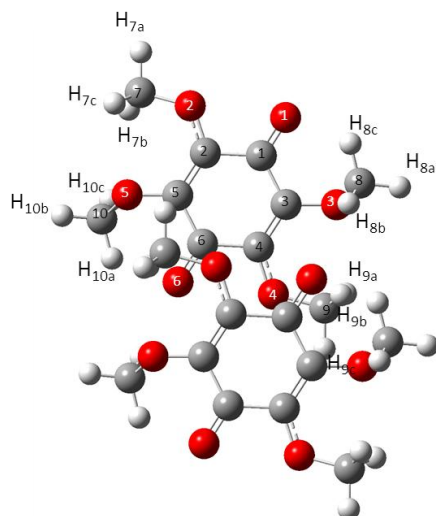
b)

	B3PW91/6-311+G(2d,p)	
angles	Dimer 1	Dimer 2
	(°)	
$\alpha(\text{O}_1\text{C}_1\text{C}_2)$	119.3	119.30
$\alpha(\text{O}_1\text{C}_1\text{C}_3)$	121.0	120.94
$\alpha(\text{O}_2\text{C}_2\text{C}_1)$	110.4	110.65
$\alpha(\text{O}_2\text{C}_2\text{C}_5)$	129.4	129.26
$\alpha(\text{O}_3\text{C}_3=\text{C}_4)$	122.3	122.70
$\alpha(\text{O}_4\text{C}_4=\text{C}_3)$	129.5	129.53
$\alpha(\text{O}_4\text{C}_4\text{C}_6)$	110.5	110.50
$\alpha(\text{O}_6\text{C}_6\text{C}_4)$	119.4	119.58
$\alpha(\text{O}_6\text{C}_6\text{C}_5)$	120.6	120.47
$\alpha(\text{O}_5\text{C}_5\text{C}_2)$	122.5	122.37
$\alpha(\text{O}_5\text{C}_5\text{C}_6)$	129.4	117.18
$\alpha(\text{C}_2\text{C}_1\text{C}_3)$	119.8	119.73
$\alpha(\text{C}_1\text{C}_3=\text{C}_4)$	120.0	120.04
$\alpha(\text{C}_6\text{C}_4=\text{C}_3)$	120.0	119.97
$\alpha(\text{C}_4\text{C}_6\text{C}_5)$	120.0	119.91
$\alpha(\text{C}_6\text{C}_5=\text{C}_2)$	119.9	119.95
$\alpha(\text{C}_7\text{O}_2\text{C}_2)$	122.8	122.53
$\alpha(\text{C}_8\text{O}_3\text{C}_3)$	117.0	116.10
$\alpha(\text{C}_9\text{O}_4\text{C}_4)$	122.9	122.64
$\alpha(\text{C}_{10}\text{O}_5\text{C}_5)$	116.6	116.59
$\alpha(\text{C}_7\text{O}_2\text{C}_2\text{C}_1)$	173.1	169.10
$\alpha(\text{C}_8\text{O}_3\text{C}_3\text{C}_1)$	66.9	69.41
$\alpha(\text{C}_9\text{O}_4\text{C}_4\text{C}_6)$	170.5	178.09
$\alpha(\text{C}_{10}\text{O}_5\text{C}_5\text{C}_6)$	68.0	67.41

Table S4: Structural parameters: a) interatomic distances and b) bond angles / dihedral angles of TMQ dimers in gas phase calculated at the B3PW91/6-311+G(2d,p) computational level. Atoms labeling used for dimer 1 and dimer 2 in this Table are displayed below on their optimized geometries.



Dimer 1



Dimer 2

Infrared		Raman		Mode description
ν_{harm} (cm ⁻¹)	Intensity (km.mol ⁻¹)	ν_{harm} (cm ⁻¹)	Intensity (Å ⁴ .amu ⁻¹)	
3151.6	20.9	3151.5	144.7 (0.750)	asym. CH stretches
3150.3	22.9	3150.3	175.1 (0.531)	
3134.5	50.7	3134.6	166.8 (0.564)	
3115.2	43.6	3115.1	119.5 (0.440)	
3052.0	108.7	3052.2	408.1 (0.036)	sym. CH stretches
3028.9	128.2	3029.1	256.1 (0.043)	
1717.1	540.0	1723.5	183.0 (0.201)	stretching $\nu_{\text{C=O}} \otimes \nu_{\text{CC}}$ ^a
1642.6	423.1	1700.1	276.6 (0.147)	stretching ν_{CC} (ring def.)
1502.3	30.0	1502.4	14.6 (0.709)	asym. bending deformation $\delta_{\text{CH}}(\text{CH}_3)$
1488.2	92.0	1489.1	14.4 (0.748)	
1480.9	14.7	1481.1	1481.1 (0.748)	
1485.5	61.5	1485.7	13.7 (0.563)	sym. bending deformation $\delta_{\text{CH}}(\text{CH}_3)$
1478.5	44.4	1479.1	14.1 (0.675)	
1460.7	52.3	1463.3	10.2 (0.299)	
1386.5	74.8	1329.7	66.5 (0.750)	$\nu_{\text{CC}}(\text{ring def.}) \otimes \delta_{\text{CH}}(\text{CH}_3)$ ^b
1329.0	965.2	1315.3	60.7 (0.722)	
		1225.1	3.1 (0.406)	
1210.4	87.8	1189.9	2.8 (0.717)	$\nu_{\text{C-O}_{(\text{CH}_3)}} \otimes \text{rocking } \delta_{\text{CH}}(\text{CH}_3)$ ^c
1197.9	39.6	1176.9	7.3 (0.573)	
1164.4	19.4	1164.0	4.3 (0.590)	rocking $\delta_{\text{CH}}(\text{CH}_3)$
1164.0	27.3	1162.5	4.8 (0.597)	
1134.1	91.2	1015.7	21.6 (0.206)	$\delta_{\text{CC}}(\text{ring def.}) \otimes \nu_{\text{O-C}_{(\text{CH}_3)}}$ ^d
1094.5	390.0	954.3	45.8 (0.737)	
967.3	121.9			
932.3	106.3			
781.4	42.9	840.7	5.4 (0.376)	o.p. bending δ_{CCC}
686.3	1.3			
		836.1	0.8 (0.648)	sym. ring def. δ_{CCC}
599.0	7.6			i.p. bending δ_{CCC}
		590.3	4.7 (0.150)	o.p. bending δ_{CCC}

^a $\nu_{\text{C=O}} \otimes \nu_{\text{CC}}$: C=O and CC (ring def.) stretches are coupled. ^b ring CC stretch coupled with bending modes $\delta_{\text{CH}}(\text{CH}_3)$. ^c C-O stretch of methoxy groups and rocking modes of CH_3 can be coupled. ^d C-O stretch of methoxy groups and δ_{CC} ring deformation are coupled.

Table S5: Calculated vibrational wavenumbers and intensities associated with the main IR-active and Raman-active vibrations of isolated TMQ in the gas phase calculated at the B3PW91/6-311+G(2d,p) level and their assignments.

assignment	Side-by side dimer 1 (TMQ) ₂				Stacked dimer 2 (TMQ) ₂			
	IR spectrum		Raman spectrum		IR spectrum		Raman spectrum	
	v _{harm} (cm ⁻¹)	Intensity (km.mol ⁻¹)	v _{harm} (cm ⁻¹)	Intensity (Å ⁴ .amu ⁻¹)	v _{harm} (cm ⁻¹)	Intensity (km.mol ⁻¹)	v _{harm} (cm ⁻¹)	Intensity (Å ⁴ .amu ⁻¹)
asym. CH stretches	3169.7	23.9	3169.7	487.4 (0.491)	3153.6	18.9	3153.6	160.9 (0.636)
	3154.2	20.6	3154.2	168.9 (0.651)	3152.5	26.8	3152.4	116.5 (0.738)
	3151.1	15.8	3151.1	128.4 (0.634)	3149.3	17.8	3149.3	114.4 (0.579)
	3149.3	18.7	3149.3	124.1 (0.608)	3147.4	20.1	3147.4	133.1 (0.610)
	3136.3	32.5	3136.1	144.5 (0.387)	3144.1	27.3	3144.2	63.3 (0.731)
	3132.2	42.4	3132.2	122.1 (0.514)	3130.3	42.2	3130.3	120.9 (0.494)
	3113.7	55.5	3113.7	160.5 (0.308)	3120.9	36.4	3121.0	113.4 (0.551)
sym. CH stretches	3112.0	47.9	3112.0	151.2 (0.324)	3111.8	45.8	3111.8	
	3049.7	98.3	3050.1	701.6 (0.050)	3057.5	70.8	3057.4	334.9 (0.049)
	3049.4	47.2	3049.6	84.4 (0.072)	3047.3	105.0	3047.3	342.1 (0.048)
	3018.2	102.4	3018.2	318.1 (0.034)	3033.8	79.8	3033.7	341.7 (0.039)
stretching(v _{C=O} ⊗v _{CC})	3016.8	147.3	3016.8	179.6 (0.049)	3017.5	138.0	3017.6	267.8 (0.063)
	1741.6	103.6	1741.6	274.5 (0.231)	1743.2	168.5	1743.4	204.3 (0.228)
stretching v _{CC} (ring def.)	1731.6	852.6	1730.2	23.3 (0.264)	1730.6	723.8	1726.8	25.8 (0.227)
	1699.7	2.1	1696.9	724.8 (0.143)	1700.8	6.2	1698.7	612.9 (0.101)
asym. bending deformation δ _{CH(CH₃)}	1654.3	1523.1	1658.4	5.0 (0.353)	1658.0	1291.5	1657.1	2.5 (0.584)
	1506.5	39.4	1505.7	17.9 (0.628)	1506.9	24.4	1506.7	21.7 (0.562)
	1504.4	18.5	1504.4	9.2 (0.713)	1504.4	21.8	1504.3	8.8 (0.724)
	1500.5	17.9	1498.9	15.6 (0.746)	1488.5	24.6	1488.7	15.3 (0.749)
	1486.5	23.6	1486.5	17.4 (0.741)	1485.9	18.2	1485.8	11.5 (0.734)
	1477.4	9.5	1477.6	15.1 (0.747)	1483.0	23.9	1483.0	13.3 (0.737)
	1476.8	18.1	1476.8	12.1 (0.715)	1477.3	13.3	1477.5	16.0 (0.691)
sym. bending deformation δ _{CH(CH₃)}	1497.9	63.5	1496.5	6.4 (0.749)	1494.6	44.3	1494.9	3.3 (0.633)
	1490.5	56.9	1490.5	7.8 (0.749)	1490.4	85.5	1490.0	10.9 (0.742)
	1481.1	2.7	1481.1	12.0 (0.610)	1480.7	10.6	1480.5	10.1 (0.581)
	1479.4	39.5	1479.4	1.1 (0.731)	1479.3	31.7	1478.9	2.8 (0.588)
	1459.4	7.2	1459.7	17.7 (0.336)	1462.7	31.7	1462.1	17.4 (0.346)
v _{CC} (ring def.)⊗v _{C-O(CH₃)}	1457.1	136.4	1457.5	1.9 (0.343)	1457.5	92.6	1457.8	5.1 (0.379)
	1346.4	13.3	1346.4	4.9 (0.599)	1346.0	22.4	1346.3	3.4 (0.746)
	1335.8	2.6	1339.6	140.5 (0.725)	1336.4	3.6	1375.7	124.7 (0.733)
	1314.6	1537.8	1321.3	3.9 (0.742)	1317.0	1263.9	1315.8	0.8 (0.745)
rocking δ _{CH(CH₃)}	1296.3	10.9	1294.8	29.1 (0.687)	1295.9	5.9	1294.4	17.8 (0.687)
	1231.2	3.3	1231.8	14.3 (0.492)	1232.6	0.4	1233.2	11.2 (0.405)
	1221.4	201.7	1221.5	0.8 (0.489)	1223.6	130.3	1223.2	0.2 (0.680)
	1209.7	119.3	1210.2	0.5 (0.718)	1210.7	108.6	1210.5	0.1 (0.134)
	1199.6	4.8	1200.2	25.2 (0.729)	1199.9	0.9	1200.1	16.4 (0.750)
	1170.9	2.7	1171.0	4.0 (0.718)	1169.1	8.3	1169.2	7.1 (0.647)
	1168.3	1.6	1168.5	13.4 (0.604)	1167.6	5.8	1167.5	4.3 (0.746)
	1166.1	1.7	1166.1	2.9 (0.594)	1166.8	5.8	1166.9	4.0 (0.590)
	1162.6	41.8	1162.7	0.3 (0.319)	1165.2	9.2	1165.3	5.7 (0.499)
	1162.0	1.5	1161.9	9.7 (0.504)	1161.9	11.7	1162.1	4.4 (0.456)
δ _{CC} (ring def.)⊗v _{CO(CH₃)}	1126.1	1165.0	1123.9	0.3 (0.645)	1125.6	1136.3	1121.1	0.1 (0.266)
	1097.2	167.1	1097.1	0.4 (0.518)	1097.2	97.2	1096.5	0.3 (0.750)
	1010.0	16.0	1009.7	31.2 (0.152)	1010.4	0.4	1010.1	29.8 (0.147)
	1004.7	54.8	1004.9	10.5 (0.142)	1005.0	83.7	1005.0	0.1 (0.735)
	972.6	1.8	972.1	55.5 (0.702)	971.4	1.8	972.5	47.4 (0.631)
sym. ring def. δ _{CCC} coupled with o.p. bending δ _{CCC}	897.8	93.5	899.2	0.3 (0.524)	899.3	81.5	899.9	0.3 (0.548)
	846.9	0.1	846.9	6.8 (0.394)	845.6	0.6	845.5	6.8 (0.364)
	831.8	0.2	831.5	7.7 (0.732)	829.9	0.3	829.9	6.7 (0.740)
o.p. bending δ _{CCC}	787.3	33.1	787.2	0.1 (0.383)	787.5	30.7	786.7	0.1 (0.658)
	689.6	26.3	6897	~0	690.4	16.9	690.3	0.1 (0.547)
i.p. bending δ _{CCC}	612.1	17.0	611.7	0.1 (0.563)	611.7	18.4	611.8	0.1 (0.240)
o.p. ring def. δ _{CCC}	575.6	0.1	575.7	15.9 (0.194)	578.1	1.4	578.4	8.6 (0.147)
	537.4	0.8	537.6	24.2 (0.137)	534.5	1.2	535.1	22.0 (0.130)

Table S6: Calculated vibrational wavenumbers and intensities associated with the main IR-active and Raman-active vibrations of TMQ in side-by-side dimer 1 and stacked dimer 2 conformations at the B3PW91/6-311+G(2d,p) level and their assignments.

	<i>a</i> (Å)	<i>b</i> (Å)	<i>c</i> (Å)	β (°)	<i>V</i> (Å ³)	<i>d</i> (Å)
corr-PBE-D* _0.52 (VASP)	3.8413 -4.08%	6.8530 -10.93%	19.1766 +13.93%	88.70 -5.67%	504.69 -2.45%	3.14 -10.03%
corr-B3PW91-D* _0.52 (CRYSTAL09)	3.7542 -6.54%	6.7768 -11.36%	19.2285 +14.48%	87.05 -9.54%	488.56 -4.73%	3.04 -12.64%
corr-PBE-D* _0.52 (CRYSTAL09)	3.7617 -4.36%	6.7883 -11.01%	19.0449 +13.66%	86.66 -7.80%	485.49 -3.19%	3.06 -8.93%
PBE-TS (CASTEP)	3.8797 -0.87%	6.7795 -12.04%	19.1872 +13.80%	90.73 -4.17%	504.63 -0.45%	3.24 -4.99%

Table S7 : Optimized lattice parameters, *a*, *b*, *c*, and β monoclinic angle, unit cell volume, V, and inter-plane distance, d, for the most stable relaxed phase of LiTMQ by using various methods of calculations. Evolution with respect to the TMQ crystal is highlighted in bold.

Theoretical calculation			
	TMQ <i>from CRYSTAL09</i> corr-B3PW91-D*_0.52 (Å)	LiTMQ <i>from CRYSTAL09</i> corr-B3PW91-D*_0.52 (Å)	Relative changes (%)
<i>d(C-C)</i>			
<i>d(C₁-C₂)</i>	1.509	1.452	-3.78
<i>d(C₂-C₃)</i>	1.362	1.374	+0.88
<i>d(C₃-C₁)</i>	1.468	1.441	-1.84
<i><d(C-C)></i>	1.446	1.422	-1.66
<i>d(C-O)</i>			
<i>d(C₄-O₂)</i>	1.439	1.428	-0.76
<i>d(C₅-O₃)</i>	1.436	1.425	-0.77
<i>d(C₁-O₁)</i>	1.227	1.270	+3.50
<i>d(C₂-O₂)</i>	1.324	1.365	+3.10
<i>d(C₃-O₃)</i>	1.362	1.373	+0.81
<i><d(C-O)></i>	1.358	1.372	+1.03
<i>d(C-H)</i>			
<i>d(C₄-H_{4a})</i>	1.088	1.089	+0.09
<i>d(C₄-H_{4b})</i>	1.090	1.091	+0.09
<i>d(C₄-H_{4c})</i>	1.089	1.087	-0.18
<i>d(C₅-H_{5a})</i>	1.090	1.093	+0.28
<i>d(C₅-H_{5b})</i>	1.093	1.092	-0.09
<i>d(C₅-H_{5c})</i>	1.093	1.093	+0.00
<i><d(C-H)></i>	1.091	1.091	+0.00
<i>d(O···H^{methyl})</i>			
<i>d(O₁···H_{5a})</i>	2.390	4.219	+76.53
<i>d(O₁···H_{4a})</i>	2.411	2.294	-4.85
<i>d(O₁···H_{5b})</i>	2.669	3.161	+18.43
<i>d(O₂···H_{4a})</i>	2.429	4.163	+71.39
<i>d(O₃···H_{5b})</i>	2.506	2.446	-2.39
<i><d(O···H^{methyl})></i>	2.481	3.257	+31.28
<i>d(Li···O)</i>			
Li···O ₁	—	1.900	
Li···O ₂	—	1.994	
Li···O ₂	—	2.914	

Table S8 : Comparison of the calculated intramolecular and intermolecular bond distances for the TMQ/LiTMQ crystals at the corr-B3PW91-D*_0.52/6-31G(d,p) level of theory.

Bond Label	R_{A-B} (Å)	BPL_{A-CP} (Å)	BPL_{B-CP} (Å)	ρ (e.Å ⁻³)	$\nabla^2\rho$ (e.Å ⁻⁵)	λ_1 (e.Å ⁻⁵)	λ_2 (e.Å ⁻⁵)	λ_3 (e.Å ⁻⁵)	$ \lambda_1 /\lambda_3$	ε
C-C										
C ₁ -C ₂	1.509 1.452	0.746 0.711	0.764 0.742	1.782 1.957	-15.905 -18.580	-13.086 -14.820	-11.784 -12.362	8.989 8.603	1.46 1.72	0.11 0.20
C ₂ -C ₃	1.362 1.374	0.702 0.703	0.611 0.673	2.247 2.193	-23.038 -21.977	-17.664 -17.134	-12.363 -12.097	6.965 7.254	2.54 2.36	0.43 0.42
C ₃ -C ₁	1.468 1.441	0.742 0.724	0.727 0.717	1.903 1.984	-17.520 -18.893	-14.242 -15.110	-12.049 -12.242	8.772 8.483	1.63 1.78	0.18 0.23
C-O										
C ₁ -O ₁	1.227 1.271	0.403 0.418	0.823 0.852	2.652 2.409	6.916 -1.325	-23.737 -20.098	-22.821 -19.278	53.475 38.051	0.44 0.53	0.04 0.04
C ₂ -O ₂	1.324 1.365	0.434 0.449	0.891 0.917	2.092 1.883	-3.374 -4.338	-15.833 -12.917	-15.592 -12.627	28.051 21.206	0.56 0.61	0.01 0.02
C ₃ -O ₃	1.362 1.373	0.454 0.456	0.909 0.918	1.963 1.896	-9.131 -7.880	-14.086 -13.158	-13.664 -12.820	18.619 18.098	0.76 0.73	0.03 0.03
C ₄ -O ₂	1.436 1.428	0.476 0.475	0.961 0.954	1.566 1.606	-4.362 -5.326	-8.724 -9.326	-8.507 -9.157	12.869 13.133	0.68 0.71	0.03 0.02
C ₅ -O ₃	1.439 1.425	0.487 0.484	0.953 0.942	1.599 1.680	-7.928 -9.615	-9.399 -10.555	-9.302 -10.193	10.748 11.157	0.87 0.95	0.01 0.04
C-H										
C ₄ -H _{4a}	1.088 1.089	0.703 0.697	0.362 0.369	1.977 1.964	-27.015 -26.339	-19.761 -19.423	-18.893 -18.580	11.664 11.663	1.70 1.67	0.05 0.05
C ₄ -H _{4b}	1.090 1.091	0.693 0.693	0.376 0.377	1.937 1.937	-25.328 -25.183	-18.942 -18.845	-18.050 -18.001	11.664 11.663	1.62 1.62	0.05 0.05
C ₄ -H _{4c}	1.089 1.088	0.694 0.691	0.374 0.376	1.950 1.957	-25.665 -25.664	-19.134 -19.110	-18.243 -18.266	11.712 11.712	1.63 1.63	0.05 0.05
C ₅ -H _{5a}	1.090 1.093	0.695 0.686	0.374 0.386	1.944 1.916	-25.665 -24.411	-19.062 -18.387	-18.170 -17.519	11.567 11.519	1.65 1.60	0.05 0.05
C ₅ -H _{5b}	1.093 1.093	0.699 0.696	0.373 0.375	1.937 1.937	-25.376 -25.207	-18.893 -18.797	-18.074 -18.025	11.591 11.615	1.63 1.62	0.05 0.04
C ₅ -H _{5c}	1.093 1.094	0.693 0.694	0.378 0.378	1.930 1.923	-24.918 -24.821	-18.725 -18.628	-17.833 -17.833	11.640 11.639	1.61 1.60	0.05 0.05

Table S9 : AIM analysis of the intramolecular interactions in the TMQ / LiTMQ (*in bold*) crystals : Calculated interatomic distance, R_{A-B} , electron density at BCP, $\rho(r)$, Laplacian of electron density at BCP, $(\nabla^2\rho(r))$, Eigenvalues of hessian of electron density, λ_1 , λ_2 and λ_3 , $|\lambda_1|/\lambda_3$ ratio and Bond Ellipticity, ε .

Bond Label	<i>G</i> (a.u.)	<i>V</i> (a.u.)	$ V /G$	<i>G/ρ</i> (a.u.)	<i>H</i> (a.u.)
C-C					
C ₁ -C ₂	0.202 0.236	-0.569 -0.665	2.817 2.816	0.765 0.815	-0.367 -0.429
C ₂ -C ₃	0.300 0.289	-0.839 -0.806	2.797 2.789	0.901 0.889	-0.539 -0.517
C ₃ -C ₁	0.227 0.243	-0.636 -0.681	2.801 2.808	0.805 0.825	-0.409 -0.438
C-O	0.000				
C ₁ -O ₁	0.653 0.507	-1.235 -1.027	1.890 2.027	1.662 1.419	-0.582 -0.520
C ₂ -O ₂	0.384 0.312	-0.804 -0.669	2.091 2.144	1.240 1.119	-0.420 -0.357
C ₃ -O ₃	0.304 0.292	-0.702 -0.665	2.312 2.280	1.043 1.038	-0.398 -0.373
C ₄ -O ₂	0.221 0.226	-0.488 -0.506	2.204 2.245	0.954 0.948	-0.267 -0.280
C ₅ -O ₃	0.206 0.216	-0.494 -0.532	2.400 2.461	0.868 0.869	-0.288 -0.316
C-H	0.000				
C ₄ -H _{4a}	0.184 0.185	-0.649 -0.643	3.521 3.478	0.629 0.635	-0.465 -0.458
C ₄ -H _{4b}	0.183 0.184	-0.630 -0.630	3.432 3.416	0.639 0.643	-0.447 -0.446
C ₄ -H _{4c}	0.185 0.187	-0.637 -0.641	3.438 3.421	0.641 0.646	-0.452 -0.454
C ₅ -H _{5a}	0.183 0.183	-0.633 -0.620	3.453 3.381	0.636 0.646	-0.450 -0.437
C ₅ -H _{5b}	0.183 0.184	-0.629 -0.630	3.438 3.419	0.638 0.642	-0.446 -0.446
C ₅ -H _{5c}	0.184 0.183	-0.627 -0.623	3.404 3.410	0.644 0.641	-0.443 -0.440

Table S10 : Kinetic energy density *G*, potential energy density *V* and $|V|/G$ ratio, *G/ρ* ratio and total energy density *H* from the AIM analysis of the intramolecular interactions in the TMQ / LiTMQ (*in bold*) crystals.

Bond Label	R _{A-B} (Å)	BPL _{A-CP} (Å)	BPL _{B-CP} (Å)	ρ (e.Å ⁻³)	$\nabla^2\rho$ (e.Å ⁻⁵)	λ_1 (e.Å ⁻⁵)	λ_2 (e.Å ⁻⁵)	λ_3 (e.Å ⁻⁵)	$ \lambda_1 /\lambda_3$	ϵ
C···O										
C ₄ ···O ₃ -C ₃ (intra)	2.808 2.770	1.446 1.540	1.408 1.384	0.094 0.101	1.325 1.470	-0.241 -0.313	-0.145 -0.145	1.711 1.928	0.14 0.16	0.67 1.24
C···H										
C ₁ ···H _{5c} -C ₅ (intra)	2.883	1.453	1.095	0.074	1.036	-0.265	-0.169	1.446	0.18	0.47
C ₄ ···H _{4c} -C ₄	3.015 2.713	1.771 1.716	1.233 1.112	0.027 0.047	0.337 0.627	-0.072 -0.145	-0.024 -0.048	0.458 0.819	0.17 0.18	1.17 1.49
C ₄ ···H _{5c} -C ₅	3.004	1.370	1.266	0.034	0.434	-0.096	-0.048	0.578	0.17	1.52
O···H										
O ₁ ···H _{5a} -C ₅	2.390	1.416	0.997	0.067	0.819	-0.241	-0.217	1.277	0.19	0.08
O ₁ ···H _{4a} -C ₄	2.411	1.455	0.979	0.074	0.819	-0.265	-0.241	1.350	0.20	0.08
O ₁ ···H _{4c} -C ₄	2.976	1.723	1.287	0.022	0.335	-0.049	-0.047	0.432	0.11	0.04
O ₁ ···H _{5b} -C ₅	2.669	1.573	1.121	0.047	0.578	-0.145	-0.120	0.843	0.17	0.18
O ₁ ···H _{5c} -C ₅ (intra)	2.519	1.459	1.191	0.067	1.036	-0.217	-0.072	1.350	0.17	1.69
O ₂ ···H _{4a} -C ₄	2.429	1.449	1.001	0.067	0.843	-0.241	-0.241	1.325	0.19	0.06
O ₂ ···H _{4c} -C ₄	2.845	1.617	1.415	0.036	0.521	-0.110	-0.064	0.695	0.16	0.72
O ₃ ···H _{4b} -C ₄	2.712 2.494	1.584 1.467	1.150 1.050	0.039 0.067	0.530 0.819	-0.132 -0.241	-0.117 -0.217	0.779 1.253	0.17 0.19	0.13 0.12
O ₃ ···H _{5b} -C ₅	2.506 2.446	1.502 1.462	1.026 1.008	0.061 0.067	0.723 0.819	-0.241 -0.241	-0.217 -0.217	1.181 1.301	0.20 0.19	0.08 0.13
O···Li										
O ₁ ···Li	1.900	0.732	1.168	0.229	7.302	-1.590	-1.566	10.459	0.15	0.01
O ₂ ···Li	1.994	0.766	1.228	0.155	5.253	-0.988	-0.940	7.205	0.14	0.05
H···H										
H _{4b} ···H _{5c} -C ₅	2.687	1.311	1.970	0.020	0.313	-0.048	-0.024	0.386	0.12	0.70
H _{4c} ···H _{5c} -C ₅	2.760	1.311	1.970	0.020	0.241	-0.048	-0.024	0.289	0.16	1.94
H _{5a} ···H _{5c} -C ₅	2.429 2.637	1.248 1.332	1.224 1.345	0.027 0.020	0.386 0.217	-0.096 -0.048	-0.048 -0.048	0.506 0.313	0.17 0.15	0.89 0.14
H _{4b} ···H _{5a} -C ₅	2.584	1.414	1.313	0.027	0.361	-0.072	-0.048	0.482	0.15	0.61
H _{4c} ···H _{5a} -C ₅	2.521	1.289	1.274	0.027	0.313	-0.072	-0.072	0.434	0.17	0.12

Table S11 : AIM analysis of the intermolecular interactions in the TMQ / LiTMQ (*in bold*) crystals:
 Calculated interatomic distance, R_{A-B}, electron density at BCP, $\rho(r)$, Laplacian of electron density at BCP,
 $(\nabla^2\rho(r))$, Eigenvalues of hessian of electron density, λ_1 , λ_2 and λ_3 , $|\lambda_1|/\lambda_3$ ratio and Bond Ellipticity, ϵ .

Bond Label	<i>G</i> (a.u.)	<i>V</i> (a.u.)	$ V /G$	<i>G/ρ</i> (a.u.)	<i>H</i> (a.u.)
C···O					
C ₄ ···O ₃ -C ₃ (intra)	0.011 0.013	-0.009 -0.010	0.803 0.806	0.824 0.854	0.002 0.003
C···H					
C ₁ ···H _{5c} -C ₅ (intra)	0.009	-0.007	0.767	0.795	0.002
C ₄ ···H _{4c} -C ₄	0.003 0.005	-0.002 -0.004	0.666 0.716	0.655 0.727	0.001 0.001
C ₄ ···H _{5c} -C ₅	0.003	-0.002	0.686	0.680	0.001
O···H					
O ₁ ···H _{5a} -C ₅	0.007	-0.005	0.783	0.703	0.002
O ₁ ···H _{4a} -C ₄	0.007	-0.006	0.823	0.658	0.001
O ₁ ···H _{4c} -C ₄	0.003	-0.002	0.622	0.774	0.001
O ₁ ···H _{5b} -C ₅	0.005	-0.003	0.731	0.679	0.002
O ₁ ···H _{5c} -C ₅ (intra)	0.008	-0.006	0.733	0.854	0.002
O ₂ ···H _{4a} -C ₄	0.007	-0.006	0.776	0.720	0.001
O ₂ ···H _{4c} -C ₄	0.004	-0.003	0.672	0.763	0.001
O ₃ ···H _{4b} -C ₄	0.004 0.007	-0.003 -0.005	0.691 0.783	0.727 0.703	0.001 0.002
O ₃ ···H _{5b} -C ₅	0.006 0.007	-0.005 -0.005	0.776 0.783	0.678 0.703	0.001 0.002
O···Li					
O ₁ ···Li	0.061	-0.046	0.752	1.789	0.015
O ₂ ···Li	0.042	-0.029	0.692	1.814	0.013
H···H					
H _{4b} ···H _{5c} -C ₅	0.002	-0.001	0.613	0.790	0.001
H _{4c} ···H _{5c} -C ₅	0.002	-0.001	0.643	0.622	0.001
H _{5a} ···H _{5c} -C ₅	0.003 0.002	-0.002 -0.001	0.647 0.657	0.740 0.566	0.001 0.001
H _{4b} ···H _{5a} -C ₅	0.003	-0.002	0.656	0.696	0.001
H _{4c} ···H _{5a} -C ₅	0.002	-0.002	0.677	0.613	0.001

Table S12 : Kinetic energy density *G*, potential energy density *V*, $|V|/G$ ratio, *G/ρ* ratio and total energy density *H* from the AIM analysis of the intermolecular interactions in the TMQ / LiTMQ (*in bold*) crystals.

Bond Label	R _{A-B} (Å)	BPL _{A-CP} (Å)	BPL _{B-CP} (Å)	ρ (e.Å ⁻³)	$\nabla^2\rho$ (e.Å ⁻⁵)	λ_1 (e.Å ⁻⁵)	λ_2 (e.Å ⁻⁵)	λ_3 (e.Å ⁻⁵)	$ \lambda_1 /\lambda_3$	ε
C-C										
C ₁ -C ₂	1.496 1.427	0.740 0.727	0.756 0.701	1.807 2.039	-16.074 -20.575	-13.278 -16.400	-11.760 -13.056	8.965 8.882	1.48 1.85	0.13 0.26
C ₂ -C ₃	1.363 1.376	0.693 0.691	0.671 0.685	2.263 2.240	-23.250 -24.485	-18.119 -18.765	-12.709 -13.728	7.579 8.008	2.39 2.34	0.43 0.37
C ₃ -C ₁	1.478 1.432	0.742 0.711	0.736 0.721	1.862 2.025	-16.832 -20.422	-13.901 -16.311	-11.872 -13.182	8.941 9.071	1.56 1.80	0.17 0.24
C-O										
C ₁ -O ₁	1.227 1.290	0.405 0.441	0.822 0.849	2.665 2.383	4.317 -14.223	-24.083 -20.393	-22.760 -19.329	51.160 25.499	0.47 0.80	0.06 0.06
C ₂ -O ₂	1.340 1.404	0.443 0.475	0.897 0.929	2.033 1.772	-5.624 -9.998	-15.024 -12.333	-14.672 -11.448	24.073 13.783	0.62 0.89	0.02 0.06
C ₃ -O ₃	1.354 1.361	0.451 0.465	0.903 0.896	2.003 2.014	-8.661 --14.098	-14.555 -15.458	-14.217 -15.047	20.111 16.407	0.72 0.94	0.02 0.03
C ₄ -O ₂	1.432 1.435	0.483 0.500	0.949 0.936	1.614 1.664	-7.198 -12.259	-9.659 -11.232	-9.607 -10.799	12.068 9.722	0.80 1.15	0.01 0.04
C ₅ -O ₃	1.430 1.420	0.486 0.494	0.943 0.926	1.646 1.734	-8.844 -13.285	-10.217 -11.983	-9.988 -11.707	11.360 10.405	0.90 1.15	0.02 0.02
O···Li										
O ₁ ···Li	1.770	1.101	0.668	0.319	9.324	-2.275	-2.152	13.751	0.165	0.06
O ₂ ···Li	1.905	1.187	0.718	0.214	5.756	-1.382	-1.263	8.401	0.165	0.05

Table S13 : AIM analysis of the intramolecular/intermolecular interactions in the TMQ / LiTMQ (*in bold*) molecular systems: Calculated interatomic distance, R_{A-B}, electron density at BCP, $\rho(r)$, Laplacian of electron density at BCP, ($\nabla^2\rho(r)$), Eigenvalues of hessian of electron density, λ_1 , λ_2 and λ_3 , $|\lambda_1|/\lambda_3$ ratio and Bond Ellipticity, ε . For the sake of simplicity and due to the rotation effect of methyl groups, bonding involving H atoms were not mentioned.

References

1. G. Kresse and J. Furthmüller, *Phys. Rev. B*, 1996, **54**, 11169.
2. S. J. Clark, M. D. Segall, C. J. Pickard, P. J. Hasnip, M. I. J. Probert, K. Refson and M. C. Payne, *Z. Kristall.*, 2005, **220**, 567.
3. R. Dovesi, R. Orlando, B. Civalleri, C. Roetti, V. R. Saunders and C. M. Zicovich-Wilson, *Z. Kristall.*, 2005, **220**, 571.
4. R. Dovesi, V. R. Saunders, C. Roetti, R. Orlando, C. M. Zicovich-Wilson, P. F. B. Civalleri, K. Doll, N. M. Harrison, I. J. Bush, P. D'Arco and M. Llunell, *CRYSTAL09 User's Manual*, University of Torino, Torino, 2009.
5. P. E. Blöchl, *Phys. Rev. B*, 1994, **50**, 17953.
6. H. J. Monkhorst and J. D. Pack, *Phys. Rev. B*, 1976, **13**, 5188.
7. S. Grimme, *J. Comput. Chem.*, 2006, **27**, 1787.
8. B. Civalleri, C. M. Zicovich-Wilson, L. Valenzano and P. Ugliengo, *CrystEngComm*, 2008, **10**, 405.
9. P. Ugliengo, C. M. Zicovich-Wilson, S. Tosoni and B. Civalleri, *J. Mater. Chem.*, 2009, **19**, 2564.
10. A.-L. Barrès, J. Geng, G. Bonnard, S. Renault, S. Gottis, O. Mentré, C. Frayret, F. Dolhem and P. Poizot, *Chem. Eur. J.*, 2012, **18**, 8800.
11. C. Frayret, E. I. Izgorodina, D. R. MacFarlane, A. Villesuzanne, A.-L. Barrès, O. Politano, D. Rebeix and P. Poizot, *Phys. Chem. Chem. Phys.*, 2012, **14**, 11398.
12. G. Bonnard, A.-L. Barrès, O. Mentré, D. G. Allis, C. Gatti, P. Poizot and C. Frayret, *CrystEngComm*, 2013, **15**, 2809.
13. A. D. Becke, *J. Chem. Phys.*, 1993, **98**, 5648.
14. W. J. Hehre, R. Ditchfield and J. A. Pople, *J. Chem. Phys.*, 1972, **56**, 2257.
15. D. Feller, *J. Comput. Chem.*, 1996, **17**, 1571.
16. K. L. Schuchardt, B. T. Didier, T. Elsethagen, L. Sun, V. Gurumoorthi, J. Chase, J. Li and T. L. Windus, *J. Chem. Inf. Model.*, 2007, **47**, 1045.
17. J. P. Perdew and Y. Wang, *Phys. Rev. B*, 1992, **45**, 13244.
18. J. P. Perdew, *Electronic Structure of Solids*, P. Ziesche, H. Eschrig edn., Akademie Verlag: Berlin, 1991.
19. F. Pascale, C. M. Zicovich-Wilson, F. López Gejo, B. Civalleri, R. Orlando and R. Dovesi, *J. Comput. Chem.*, 2004, **25**, 888.
20. C. M. Zicovich-Wilson, F. Pascale, C. Roetti, V. R. Saunders, R. Orlando and R. Dovesi, *J. Comput. Chem.*, 2004, **25**, 1873.
21. A. Tkatchenko and M. Scheffler, *Phys. Rev. Lett.*, 2009, **102**, 073005.
22. M. J. Frisch, G. W. Trucks, H. B. Schlegel, G. E. Scuseria, M. A. Robb, J. R. Cheeseman, G. Scalmani, V. Barone, B. Mennucci, G. A. Petersson, H. Nakatsuji, M. Caricato, X. Li, H. P. Hratchian, A. F. Izmaylov, J. Bloino, G. Zheng, J. L. Sonnenberg, M. Hada, M. Ehara, K. Toyota, R. Fukuda, J. Hasegawa, M. Ishida, T. Nakajima, Y. Honda, O. Kitao, H. Nakai, T. Vreven, J. Montgomery, J. A., J. E. Peralta, F. Ogliaro, M. Bearpark, J. J. Heyd, E. Brothers, K. N. Kudin, V. N. Staroverov, R. Kobayashi, J. Normand, K. Raghavachari, A. Rendell, J. C. Burant, S. S. Iyengar, J. Tomasi, M. Cossi, N. Rega, J. M. Millam, M. Klene, J. E. Knox, J. B. Cross, V. Bakken, C. Adamo, J. Jaramillo, R. Gomperts, R. E. Stratmann, O. Yazyev, A. J. Austin, R. Cammi, C. Pomelli, J. W. Ochterski, R. L. Martin, K. Morokuma, V. G. Zakrzewski, G. A. Voth, P. Salvador, J. J. Dannenberg, S. Dapprich, A. D. Daniels, Ö. Farkas, J. B. Foresman, J. V. Ortiz, J. Cioslowski and D. J. Fox, *Gaussian09*, 2009.
23. Frayret, C.; Izgorodina, E. I.; MacFarlane, D. R.; Villesuzanne, A.; Barrès, A.-L.; Politano, O.; Rebeix, D.; Poizot, P. *Phys. Chem. Chem. Phys.*, 2012, **14**, 11398.

24. A. Julg and P. François, *Theor. Chem. Acta*, 1967, **8**, 249.
25. E. Matito, M. Duran and M. Sola, *J. Chem. Phys.*, 2005, **122**, 014109.
26. E. Matito, M. Duran and M. Sola, *J. Chem. Phys.*, 2006, **125**, 059901.
27. R. F. W. Bader, *Atoms in Molecules: A Quantum Theory*, Clarendon Press edn., Oxford, 1990.
28. X. Fradera, M. A. Austen and R. F. W. Bader, *J. Phys. Chem. A*, 1998, **103**, 304.
29. R. F. W. Bader and M. E. Stephens, *J. Am. Chem. Soc.*, 1975, **97**, 7391.